N90-23035

CONTROL OF A FLEXIBLE PLANAR TRUSS USING PROOF MASS ACTUATORS

Constantinos Minas*
Ephrahim Garcia
Daniel J. Inman
Department of Mechanical and Aerospace Engineering
State University of New York at Buffalo
Buffalo, N.Y. 14260

Abstract

A flexible structure was modelled and actively controlled by using a single space realizable linear proof mass actuator. The NASA/UVA/UB actuator was attached to a flexible planar truss structure at an "optimal" location and it was considered as both passive and active device. The placement of the actuator was specified by examining the eigenvalues of the modified model that included the actuator dynamics, and the frequency response functions of the modified system. The electronic stiffness of the actuator was specified, such that the proof mass actuator system was tuned to the fourth structural mode of the truss by using traditional vibration absorber design. The active control law was limited to velocity feedback by integrating of the signals of two accelerometers attached to the structure. The two lower modes of the closed-loop structure were placed further in the LHS of the complex plane. The theoretically predicted passive and active control law was experimentally verified.

1. Introduction

Large continuous structures, like space structures tend to have tight restrictions on the actual response of the structure. A passive or active control design is often necessary for the structure to satisfy the desired response restrictions. The success of the passive and active control design is based on the accuracy of the model that describes the dynamic characteristics of the structure. Flexible distributed parameter systems can be successfully modelled by finite element analysis [1]. This category of structures is lightly damped and tends to have most of its mass concentrated at the joints [2]. Their natural frequencies are low and appear in closely spaced groups. The finite element model of the structure that consists of a mass and a stiffness matrix, can be reduced by traditional model reduction techniques by eliminating the insignificant displacements at the nodal points [3]. The dissipation energy of the system can be modelled by constructing a system damping matrix, by assuming a normal mode system [4], and by using the damping ratios obtained experimentally from modal parameter estimation methods [5, 6, 7]. In the case where the discrepancy between the analytical model and the experimentally obtained modal model is significant, the reduced order analytical damped model can be further modified [8], such that it is in agreement with the experimental natural frequencies, damping ratios and mode shapes [8,9,10,11,12,13]. It is important to realize that the design of the "optimal" control is based on the modified reduced order model, but it is actually applied to the real structure. Therefore, the model improvement mentioned above, becomes very important and its accuracy is vital in the success of the design of the control law.

The structure used here, is a planar truss constructed with space realizable links and joints in the configuration presented in fig.1. The truss is lightly damped and has the behavior of a large

---

*Currently with G.E. Corporate Research and Development Center, Advanced Projects Laboratory, Schenectady, N.Y. 12301.

5. Nikravesh, P. E., 1984, "Some Methods for Dynamics of Constrained Mechanical Systems: A Survey", NATO ASI Series, Vol. F9, Springer-Verlag, Berlin, pp. 351-368.

6. Ider, S. K., 1988, "Stability and Dynamics of Constrained Flexible Multibody Systems", PhD Thesis, University of Illinois at Chicago.

7. Ider, S. K., Amirouche, F. M. L., 1989, "Nonlinear Modeling of Flexible Multibody Systems Dynamics Subjected to Variable Constraints" ASME Journal of Applied Mechanics, Vol. 56, No. 2, pp. 444-450.

8. Ider, S. K., Amirouche, F. M. L., 1988, "Coordinate Reduction in the Dynamics of Constrained Multibody Systems", ASME Journal of Applied Mechanics, Vol. 55, No. 4, pp. 899-905.

9. Ider, S. K., 1989, "Modeling of Control Forces for Kinematical Constraints in the Dynamics of Multibody Systems-A New Approach", 3rd Annual Conf. on Aerospace Computational Control, Oxnard, CA, Sept.

10. Przemieniecki, J. S., 1968, Theory of Matrix Structural Analysis, McGraw-Hill, New York.

11. Naganathan, G., Soni, A. H., 1986, "Nonlinear Modeling of Kinematic and Flexibility Effects in Manipulator Design", ASME Paper, 86-DET-88.

12. Kane, T. R., Ryan, R. R., Banerjee, A. K., 1987, "Dynamics of a Cantilever Beam Attached to a Moving Base", Journal of Guidance, Control and Dynamics, Vol. 10, No.2, pp. 139-151.

space structure, with most of its mass concentrated at the joints [2]. It possesses low resonant frequencies that appear in closely spaced groups and has both translational and rotational modes of vibration.

The structure is passively and actively controlled by a single actuator. The actuator used in this experiment is the NASA/UVA/UB proof mass actuator system. The actuator dynamics are taken into consideration and a global model is constructed which includes both the structure and the actuator dynamics [14,15]. The location of the actuator is specified [16,17] by examining the eigenvalues of the uncontrolled global model and the frequency response functions of the global system. The actuator is considered as both a passive and an active device with two design variables, its electronic stiffness and the generated force. The electronic stiffness is specified such that the actuator proof-mass-electronic-spring system is tuned to one of the structural modes of the truss by using traditional vibration absorber design [18,19,20]. The generated force of the actuator is specified by using output feedback techniques. Here, the active control law was limited to velocity feedback by integrating the signals of two accelerometers attached to the structure. The objective is to move the two lower modes of the closed-loop structure further in the LHS of the complex plane and at the same time maintain stability of the closed-loop system [21,22]. The theoretically predicted passive and active control law are experimentally implemented and the results are evaluated.

2. Modeling

2.1 Construction of the Finite Element Model

The finite element model of the structure was constructed by using the commercially available MSC/PAL package for dynamic modeling. The structure weighed 7.335 Kg and was constructed with links and joints, mainly made of aluminum alloy. The density of the material was measured experimentally by using standard techniques. The Young's modulus of aluminum alloy was used, since the links and joints are mainly constructed with this material. The nodal points of the finite element model coincide with the location of the joints of the structure. Every nodal point was allowed to have three degrees of freedom, that is translation in the z-axis and rotations about the x and y-axis resulting in a 48-degree-of-freedom model (see Fig.1). The boundary conditions were assumed to be clamped for nodes 15 and 16 and free for the rest of the nodes, since the structure was supported as illustrated in fig.1. After the boundary conditions were applied the final model was a 42-degree-of-freedom model.

2.2 Mass Distribution

The mass distribution of a non-uniform structure is a problem, that should by no means be ignored. Here, two approaches were used. The first approach was to calculate an equivalent internal diameter of the hollow links, such that the links had the measured mass. The links were treated as uniform hollow tubes constructed with aluminum alloy with an equivalent length of 0.5m. The joints were modelled as a concentrated mass at the particular location and are treated as rigid. The natural frequencies of this model were calculated and are presented in table 1. The results were considered unsatisfactory and one of the links was disassembled for more insight to the mass distribution of the link. In the second approach, the real internal diameter of the links was used and the excessive mass was distributed to the nodes accordingly. The resulting natural frequencies of the model are compared to the experimental results in table 1. The finite element model was constructed using a finer grid which include more nodal points, specifically an additional nodal point at the mid-point of each link. The resulting model after the boundary conditions were applied was a 126-degree-of-freedom model.

It can be concluded that the 45-node(126-dof) model is not significantly better than the 16-node(42-dof) model in predicting the first fourteen natural frequencies. Therefore, it was found unnecessary to use the 45-node(126-dof) model in the determination of the control design of the structure, since the 16-node(42-dof) model was as accurate.

Table 1 : Comparison of the theoretical and experimental natural frequencies of the structure.

FEM					TEST I (rot accel)
	Uniform mass distribution	Corrected mass distribution			
	42dof	42dof	126dof	14dof	SDOF analysis
Frequency in Hz					
1	1.38	1.045	1.048	1.039	1.07
2	4.56	3.467	3.468	3.469	3.54
3	10.88	8.050	8.050	8.051	7.94
4	26.98	19.894	19.894	19.902	-
5	29.68	21.746	21.748	21.750	-
6	30.94	22.077	22.074	22.087	22.54
7	42.63	30.468	30.472	30.477	32.61
8	53.79	39.268	39.252	39.326	40.35
9	68.46	48.524	48.521	48.552	-
10	72.61	51.746	51.704	51.842	52.51
11	82.93	58.645	58.629	58.718	61.41
12	101.93	71.169	71.116	71.275	65.62
13	102.88	72.090	72.039	72.285	78.24
14	116.52	80.741	80.610	80.920	91.74
15	236.64	219.856	183.903	-	187.13

2.3 Model Reduction

Most of the control algorithms are designed for first order systems. Transforming the 16-node(42-dof) model in the state space results in a 84-dof state space matrix. This matrix is quite large, and it was found that it is difficult to manipulate in vibration prediction, and control algorithms. Therefore, it was necessary to reduce the order of the model before performing control analysis and designing a control law. From the configuration of the model the rotational degrees of freedom can be considered as less significant than the translational ones, and can be eliminated from the model by using the Guyan reduction method [3]. The resulting reduced order model is a 14-dof model. Eigenvalue analysis of this model showed that this model maintained the first fourteen natural frequencies of the larger model quite accurately. The damping ratios determined from the modal test were used in the construction of the system's damping matrix, by assuming that the system exhibited normal mode behavior. The damping matrix is calculated by the following equation:

$$D = MU_F \mathrm{diag}(2\zeta_i\omega_i)U_F^{-1} \tag{1}$$

where U_F is the eigenvector matrix of $M^{-1}K$, and ζ_i are the experimentally obtained damping ratios. The final reduced order model is described by the following equation:

$$M\ddot{q}(t) + D\dot{q}(t) + Kq(t) = 0 \tag{2}$$

This equation describes only the dynamic characteristics of the structure. The actuator dynamics were considered important and they were included in the dynamic model.

2.4 Actuator Dynamics

The actuator that was used in this experiment was the NASA/UVA/UB proof mass actuator, presented in fig.2. The actuator system is comprised of a movable proof mass (m_{prf} = 0.225Kg), a fixed coil that applies an electromagnetic force on the proof mass, an analog interface board, a power amplifier and a linear variable differential transformer (LVDT) sensor. The LVDT transducer is an electromechanical transducer that measures the relative position of the proof mass with respect to the actuator housing. The actuator can be modelled as single degree of freedom mass-spring system, with a variable electronic stiffness and the ability to apply a force on the structure at the attachment point. An equal and opposite force is applied on the proof mass of the actuator. The actuator is space-realizable in the sense that it does not have to be attached to the ground. The equations of motion are written by taking into account the actuator dynamics[15]. Let's assume that the actuator is attached to the structure at the ith nodal point. The global system that includes both the structure and the actuator dynamics, is of higher order, equal to the order of the original system plus the order of the actuator dynamics, and it is described by:

$$\begin{bmatrix} M_1 & 0 \\ 0 & m_{prf} \end{bmatrix} \begin{bmatrix} \ddot{q} \\ \ddot{q}_{prf} \end{bmatrix} + \begin{bmatrix} D_1 & & 0 \\ & & -c_{act} \\ & & 0 \\ 0 & -c_{act} \; 0 & c_{act} \end{bmatrix} \begin{bmatrix} \dot{q} \\ \dot{q}_{prf} \end{bmatrix} + \begin{bmatrix} K_1 & & 0 \\ & & -k_{act} \\ & & 0 \\ 0 & -k_{act} \; 0 & k_{act} \end{bmatrix} \begin{bmatrix} q \\ q_{prf} \end{bmatrix} = \begin{bmatrix} 0 \\ 1 \\ 0 \\ -1 \end{bmatrix} f_g \quad (3a)$$

where q_{prf} is the displacement of the proof mass (m_{prf}), the scalars k_{act} and c_{act} are the stiffness and damping of the electronic spring of the actuator, m_{par} is the parasitic mass of the actuator, f_g is force generated by the actuator, and the matrices M_1 ,D_1 and K_1 are the following matrices:

$$M_1 = M + m_{par}\mathrm{diag}[0,\ldots,0,1,0,\ldots,0] \quad (3b)$$

$$K_1 = K + k_{act}\mathrm{diag}[0,\ldots,0,1,0,\ldots,0] \quad (3c)$$

$$D_1 = D + c_{act}\mathrm{diag}[0,\ldots,0,1,0,\ldots,0] \quad (3d)$$

This is referred to as the open-loop system and the mass, damping and stiffness matrices are denoted by subscript ($_{OL}$) for convenience. Note that the non-zero elements correspond to the ith row or/and column of the particular matrix or vector of the previous set of equations. The force f_g is the actuator-generated force applied on the structure. The electronic stiffness of the actuator can be selected in a variety of ways for various design approaches.

3. Passive Control Design

3.1 Structural Modification Design

The parasitic mass of the actuator housing has the same effect as adding a dead parasitic mass at the point of attachment. Increasing the mass of the structure is a structural modification, with the direct effect of reducing the lower natural frequencies of the system. The natural frequencies of the new model with the dead mass were examined both theoretically and experimentally, and the results are tabulated in table 2. The experimental results are presented in the form of point and transfer inertance (transfer function) plots. The transfer function of nodes 1 and 8, of both the original structure and the modified structure are presented in fig.3 and fig.4 respectively. The effect of attaching the PMA (inactive) was also examined. This configuration is equivalent of having a dead mass equal to the parasitic mass of the actuator housing plus the proof mass. However, when the actuator's electronic stiffness is activated, the proof mass becomes an additional degree of freedom, and it is not part of the parasitic mass any longer.

The results indicate that the modified structure has lower natural frequencies than the original structure. This is true for the first five structural modes as indicated in the table above. The experimental frequency response plots show that the level of the vibration response was reduced considerably, especially in the lower frequency region.

If the design methodology was limited to structural modification, it will be considered necessary to examine the effect of adding the dead mass at different nodal points. The results are presented in table 3. The design criterion that was used to place the actuator was to reduce the overall vibration level at node 1, because a sensitive device will be attached at that point. The actuator cannot be placed at node 1 because there is no room. Note that different design criterion results in different locations of the actuator. Placing the actuator at node 10 doesn't reduce the vibration at node 1 at all. Nodes 2, 3, and 4 have the same effect in reducing the vibration level of node 1. But the first structural mode is shifted at 0.92 Hz. This was considered undesirable because it is hard to control the low frequencies by active control. Placing the actuator at nodes 6,7 and 8 has the same effect in reducing the vibration level of node 1 and the first structural mode is not shifted considerably. Therefore, any of nodes 6,7, and 8 can be used as an "optimal" location of the actuator. The results that follow are for placing the actuator at node 8.

Table 2 : Comparison of the theoretical and experimental natural frequencies of the structure with and without the parasitic mass.

	FEM		TEST I		
	w/o	w	w/o	w dead mass	w PMA inactive
	Frequency in Hz				
1	1.04	0.97	1.07	1.01	1.02
2	3.47	2.94	3.54	3.09	2.96
3	8.05	8.00	7.94	7.69	7.88
4	19.90	16.42	-	17.01	16.03
5	21.75	21.44	-		22.39
6	22.09	22.06	22.54	22.02	23.50
7	30.48	28.53	32.61	30.08	29.50
8	39.33	39.12	40.35	39.78	39.33
9	48.55	46.40	-	-	-
10	51.84	51.45	52.51	49.31	50.68
11	58.72	58.52	61.41	54.57	57.36
12	71.27	70.71	65.62	65.02	66.29
13	72.28	72.28	78.24	77.73	78.41
14	80.92	80.74	91.74	84.8	-

Table 3 : Comparison of the theoretical natural frequencies of the structure with the parasitic mass at various nodal points.

	FEM								
	w/o	8	2	3	4	5	6	7	10
	Frequency in Hz								
1	1.04	0.97	0.93	0.93	0.92	0.98	0.98	0.98	1.01
2	3.47	2.94	3.39	3.40	2.94	2.96	3.41	3.40	3.42
3	8.05	8.00	7.71	7.66	7.65	7.95	7.93	7.95	7.28
4	19.90	16.42	18.25	18.41	17.47	15.54	19.84	19.88	19.52
5	21.75	21.44	21.74	21.45	20.17	21.75	20.52	20.24	20.52
6	22.09	22.06	21.98	22.07	21.77	21.96	21.94	21.75	22.00
7	30.48	28.53	30.09	30.02	29.60	27.79	30.07	30.43	29.83
8	39.33	39.12	39.17	38.15	37.87	36.87	39.30	38.92	37.06
9	48.55	46.40	45.12	46.65	48.35	48.35	43.27	45.40	43.03
10	51.84	51.45	51.67	49.02	49.76	50.89	49.56	51.40	51.83
11	58.72	58.52	54.15	57.71	58.47	58.54	58.60	56.68	56.07
12	71.27	70.71	68.85	68.34	70.27	70.62	67.91	68.31	68.53
13	72.28	72.28	71.87	72.26	72.26	72.09	71.67	72.23	71.34
14	80.92	80.74	80.44	80.13	80.69	80.67	79.27	79.27	77.81

3.2 Vibration absorber design

There are several criteria for tuning the absorber to a MDOF structure. The simplest criterion is to tune the natural frequency of the absorber to exactly one of the natural frequencies of the structure[18], that is:

$$\omega_a = \omega_i \tag{4a}$$

The design of the damped absorber results in an optimal tuned frequency given by[18]:

$$\omega_a = \frac{\omega_i}{1+\mu_i} \tag{4b}$$

where μ_i is the ratio of the mass of the absorber (here, the proof mass) over the mass of the SDOF structure (here, the modal mass at mode ω). The ratio μ_i or the modal mass can be calculated in a trial and error procedure. The difficulty of applying the second method is the fact that it is difficult to determine the optimal value for μ for the higher modes [22].

An optimal tuning criterion for MDOF systems was presented in reference [19]. The absorber frequency (ω_a) and damping coefficient (c_a) are given by:

$$\omega_a^2 = \omega_i^2 \frac{1+\mu_t}{(1+\mu_t+\mu_a)^2} \tag{5a}$$

$$c_a^2 = m_a^2\omega_i^2\mu_a \frac{1+\mu_t}{(1+\mu_t+\mu_a)^3} \tag{5b}$$

where,

$$\mu_t = m_t\phi_{i_j}^2 \text{ and } \mu_a = m_a\phi_{i_j}^2 \tag{5c}$$

The scalars m_t and m_a are the parasitic mass and the mass of the absorber, respectively, and the scalar ϕ_{i_j} is the jth entry of the associated eigenvector of the ith mode, where j is the degree of freedom corresponding to the location of the absorber. Note that the eigenvectors derived form the finite element model, are normalized with respect to the mass matrix.

3.2.2 Experimental implementation of the passive control design

The stiffness of the PMA can be electronically varied, such that the actuator system can be tuned to different frequencies. The PMA was attached to ground, and the LVDT signal was examined for random signal input that generates an electromagnetic force on the proof mass. The LVDT signal gives the relative position of the proof mass with respect to the housing of the actuator. As it can be clearly seen in the experimental bode plot in fig.5, the PMA system is well modelled by a SDOF system, with a natural frequency depending on the gain that determines the electronic stiffness. The stiffness is a function of the external gain (α), and other electromagnetic constants of the coil and the amplifier (included in the factor K) . The natural frequency of the system is given by:

$$\omega_a = 1/2\pi \sqrt{\alpha K/m_{prf}} \tag{6}$$

The damping in the actuator was identified as Coulomb damping due to the friction in the bearings. An equivalent viscous coefficient was calculated from the frequency response functions of the LVDT signal at particular tuning frequencies. It was found that the lower the tuning frequency becomes, the higher the equivalent damping becomes. This is actually due to the fact that at low frequencies the proof mass of the actuator cannot overcome the friction. As a consequence, the natural frequency of the SDOF model of the actuator dynamics cannot go lower than a certain frequency, since the stiffness is electronically determined and it depends on the relative motion of the proof mass with respect to the housing of the actuator. It was found that the actuator system behaves like an overdamped system when tuned to frequencies below 8 Hz. Therefore, it was practically impossible to tune the actuator to frequencies lower than 8 Hz. Note that, this range includes the three lower natural frequencies of the modified structure. Therefore, the PMA is tuned to the fourth mode, by using the criteria described above. The results from only the second criterion are presented here in the top part of fig.6, due to the fact that the plots from the simple criterion (equation 4a) and the optimal tuning criterion (equation 5) were very similar. It can be clearly seen that the vibration response is clearly reduced.

4. Active Control design

The active control law is implemented, by using one actuator and two sensors. The force generator signal of the actuator was then given by:

$$f_g = FCy(t) \tag{7}$$

where F the feedback gain matrix and C the output matrix. The sensors were placed at node 1 and node 4 as indicated in fig.1. Node 1 was chosen because this is the possible point of attachment of a sensitive device, where the vibration level is required to be reduced. Node 4 was chosen, because it moves in the opposite direction of node 1, when the structure is excited at one of its rotational modes. Here, accelerometers were used and their signals were integrated once by an analog computer, to give the corresponding velocity signals. The output position matrix was therefore zero, and the velocity output matrix was of the form:

$$C_1 = \begin{bmatrix} 1 & & 0_{1\times14} \\ 0_{1\times3} & 1 & 0_{1\times11} \end{bmatrix} \tag{8}$$

The gain matrix is therefore given by:

$$F = [g_1 : g_2] \tag{9}$$

where g_1 and g_2 are the two gains to be determined. Substituting into the previous equation results in:

$$f_g = F\begin{bmatrix} 1 & & 0_{1\times14} \\ 0_{1\times3} & 1 & 0_{1\times11} \end{bmatrix}\dot{q}(t) \tag{10}$$

The closed-loop system written in physical coordinate system, is given by the following equation:

$$M_{OL}\ddot{q}(t) + D_{OL}\dot{q}(t) + K_{OL}q(t) = B_{OL}FC_1\dot{q}(t) \tag{11}$$

The objective here is to calculate the gain matrix F such that the system has poles at the desired locations. The right hand side of the previous equation is expanded as:

$$B_{OL}FC_1 = \begin{bmatrix} 0 \\ 1 \\ 0 \\ -1 \end{bmatrix}[g_1 : g_2]\begin{bmatrix} 1 & & 0_{1\times14} \\ 0_{1\times3} & 1 & 0_{1\times11} \end{bmatrix} = \begin{bmatrix} & & 0_{7\times15} & & \\ g_1 & 0 & 0 & g_2 & 0_{1\times11} \\ & & 0_{6\times15} & & \\ -g_1 & 0 & 0 & -g_2 & 0_{1\times11} \end{bmatrix} \tag{12}$$

Note that this is a square sparse asymmetric matrix with only four non-zero elements. This results in a closed-loop system damping matrix of the form:

$$D_{CL} = \begin{bmatrix} D_1 & & & 0 \\ & & & -c_{act} \\ & & & 0 \\ 0 & -c_{act} & 0 & c_{act} \end{bmatrix} + \begin{bmatrix} & & 0_{7\times15} & & \\ g_1 & 0 & 0 & g_2 & 0_{1\times11} \\ & & 0_{6\times15} & & \\ -g_1 & 0 & 0 & -g_2 & 0_{1\times11} \end{bmatrix} \tag{13}$$

where c_{act}, corresponds to the equivalent viscous damping coefficient of the actuator system.

The objective here, was to decrease the amplitude of the vibration response at the low modes that have high participation factors. Note that, direct pole placement design could not be applied since with one actuator and two sensors, only one closed-loop pole can be placed. The gains were determined in an ad hoc design, from an algorithm that covered a broad region of values, with the main objective to move the lower two poles further in the LHS complex plane. The results are presented in table 6. It can be clearly seen that the closed-loop system is stable when the two gains g_1 and g_2, are in the region -10 to 10 and 0 to 15 respectively. A finer grid that covered the part of the stable region, where the damping of the first two modes was increased (g_1 from 0 to 10 and g_2 from 10 to 20) was also examined [22].

It was discovered that the "optimal" gain of F= [5 : 15] increases the damping on modes 1, 2, 4, 5, 6 and decreases the damping at mode 3. Note that, further increase of the gains towards the "optimal" direction, resulted in an unstable closed-loop system. The experimentally obtained transfer functions of nodes 1 and 8, are presented in fig.6, and they are compared directly with the open-loop system, tuned to the fourth structural mode. The results show clearly, a decrease in the response at modes 1 and 2. The decrease of the vibration response is not very large as desired, because of the following reasons:

(i) By using only one actuator and two sensors, we can only affect 4 elements of the 15x15 closed-loop damping matrix.

(ii) Further increase in the gains towards the "optimal" direction drives the third mode unstable.

(iii) We are trying to control a flexible structure with many significant modes that cannot be ignored.
(iv) We are only using velocity feedback

It was also illustrated experimentally that by increasing the gains at higher values drove the proof mass system unstable.

Table 6 : Determination of the feedback gain matrix

g_2 \ g_1	-20	-15	-10	-5	0	5	10	15	20	25	30
-20	U	U	U	U	U	U	U	U	U	U	U
-15	U	U	U	U	U	U	U	U	U	U	U
-10	U	U	U	U	U	U	U	U	U	U	U
-5	U	U	U	U	U	U	U	U	U	U	U
0	U	U	U	S	S	U	U	U	U	U	U
5	U	U	S	S	S	S	U	U	U	U	U
10	U	U	U	S	S	S	S	U	U	U	U
15	U	U	U	U	S	S	U	U	U	U	U
20	U	U	U	U	U	U	U	U	U	U	U

U = unstable, S = stable.

5. Closing Remarks

An experimental flexible planar truss structure was modelled and successfully controlled in a passive and active way by using a space realizable linear proof mass actuator system. The PMA was attached to the truss at a desired location, and tuned as traditional vibration absorber to one of the structural modes of the truss by using several criteria. The actuator dynamics were successfully modelled and taken into consideration in the design of the passive and active control law. The active control design was adopted in the form of output velocity feedback by integrating the signals of two accelerometers, attached to the structure. The limitations of this method were indicated and difficulties of applying output feedback on large flexible structures with several significant modes are identified and pointed out.

6. Acknowledgements

This work was supported in part by AFOSR grants no F49620-88-00018 and F49620-86-6-0111. Much of the equipment used was funded through instrumatation grants numbers AFOSR-85-0119 and AFOSR-88-450-0390.

7. References

(1) Shames, I.H. and Dym, C.L., 1985, Energy and Finite Element Methods in Structural Mechanics, Hemisphere Publishing Corp., Chapter 16, pp.643-657.
(2) Balas, M. J., 1982, "Trends in Large Space Structure Control Theory: Fondest hopes, Wildest Dreams," IEEE Transactions on Automatic Control, Vol. AC-27, No. 3, June, pp. 522-535.
(3) Guyan, R.J., 1965, "Reduction of Stiffness and Mass Matrices," AIAA Journal, Vol. 14, pp.1627-1628.
(4) Caughey, T.K. and O'Kelly, M.E., 1965, "Classical Normal Modes in Damped Linear Dynamic Systems," ASME Journal of Applied Mechanics, Vo. 32, pp.583-588.
(5) Ewins, D.J., 1986, Modal Testing: Theory and Practice, Research Studies Press Ltd., England.
(6) Ibrahim, S.R. and Mikulcik, E.C., 1976, "The Experimental Determination of Vibration Parameters from Time Responses," Shock and Vibration Bulletin, No. 46, pt.5, pp.187-196.
(7) Juang, J.N. and Pappa, R.S., 1985, "An Eigensystem Realization Algorithm (ERA) for Modal Parameter Identification and Model Reduction," AIAA Journal of Guidance, Control and Dynamics, vol.8, 5, Sept-Oct, pp.620-627.

(8) Kammer, D.C., 1987, "An Optimum Approximation for Residual Stiffness in Linear System Identification," Proceedings of the 28th SDM Conference, Monterey, California, pp.277-287.
(9) Berman, A., 1984, "System Identification of Structural Dynamic Models-Theoretical and Practical Bounds," Proceedings of the 25th SDM Conference, Palm Springs, California, May, pp.123-129.
(10) Berman, A. and Nagy, E.Y., 1983, "Improvement of a Large Analytical Model Using Test Data," AIAA Journal, Vol.21, Aug., pp.1168-1173.
(11) Minas, C. and Inman, D.J., 1988, "Correcting Finite Element Models with Measured Modal Results using Eigenstructure Assignment Methods," Proceedings of the 6th International Modal Analysis Conference, Orlando, Florida, February, pp.583-587.
(12) Minas, C. and Inman, D.J., 1989, "Matching Finite Element Models to Modal Data," ASME Journal of Vibration, Acoustics, Stress, and Reliability in Design, (accepted for publication, paper No. 88-487).
(13) Minas, C. and Inman, D.J., 1989, "Model Improvement by using Pole Placement Methods," Proceedings of the 12th Biennial ASME Conference in Vibration and Noise, Sept., Montreal, Canada.
(14) Zimmerman, D. C., Horner, G. C., and Inman, D. J., 1988, "Microprocessor Controlled Force Actuator," AIAA Journal of Guidance, Control, and Dynamics, Vol. 11, No. 3, May-June, pp.230-236.
(15) Harokopos, E. G. and Mayne, R. W., 1986, "Motor Characteristics in the Control of a Compliant Load," AIAA Journal of Guidance, Control, and Dynamics, Vol. 9, No. 1, Jan.-Feb., pp. 113-118.
(16) Chiang,H.D., Thorp, J.S., Wang, J.C., and Lu, J., 1989, "Optimal Controller Placements in Large Scale Linear Systems," Proceedings of the American Control Conference, pp.1615-1620.
(17) Min, I.J., Chang, and Soong,T.T., 1980, "Optimal Controller Placement in Modal Control of Complex Systems," Journal of Mathematical Analysis and Applications, Vol.75, pp.340-358.
(18) Den Hartog, 1956, Mechanical Vibrations, 4th edition, McGraw-Hill, New York.
(19) Juang, J.N., 1984, Optimal Design of a Passive Vibration Absorber for a Truss Beam," AIAA Journal of Guidance, Control and Dynamics, vol.7, 6, Nov.-Dec., pp.733-739.
(20) Miller, D.W. and Crawley, E.F., 1988, "Theoretical and Experimental Investigation of Space-Realizable Inertial Actuation for Passive and Active Structural Control," AIAA Journal of Guidance, Control and Dynamics, vol.11, 5, Sept-Oct, pp.449-458.
(21) Andry, A.N., Shapiro, E.Y., and Chung, J.C., 1983, "Eigenstructure Assignment for Linear Systems, "IEEE Transactions on Aerospace and Electronic Systems, " Vol. AES-19, no.5, September, pp.711-729.
(22) Minas, C., 1989, "Modeling and Active Control of Large Flexible Structures," Ph.d. dissertation, State University of New York at Buffalo .

443

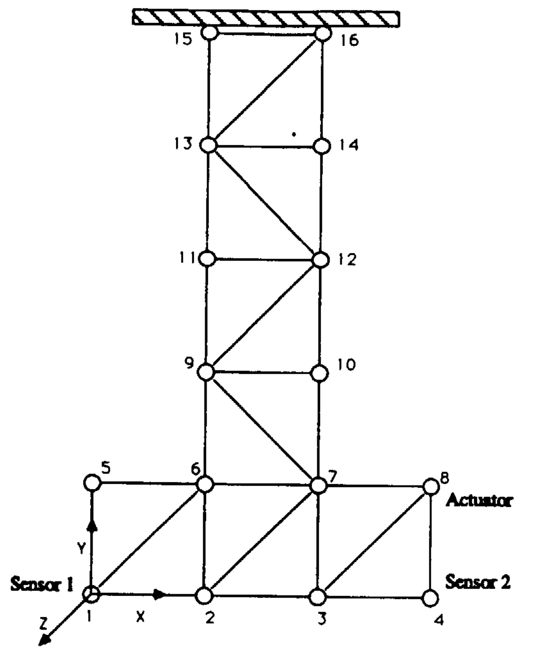

Fig.1 : Structure configuration with locations of sensors and actuator

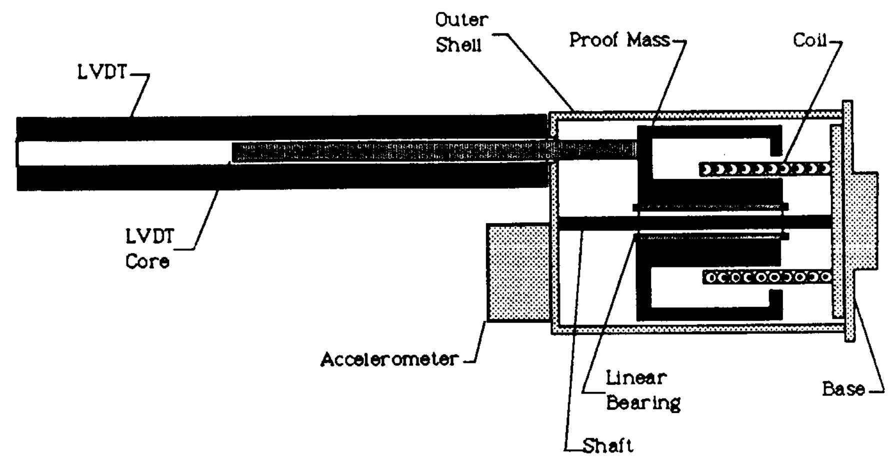

Fig 2 : Configuration of the proof mass actuator system

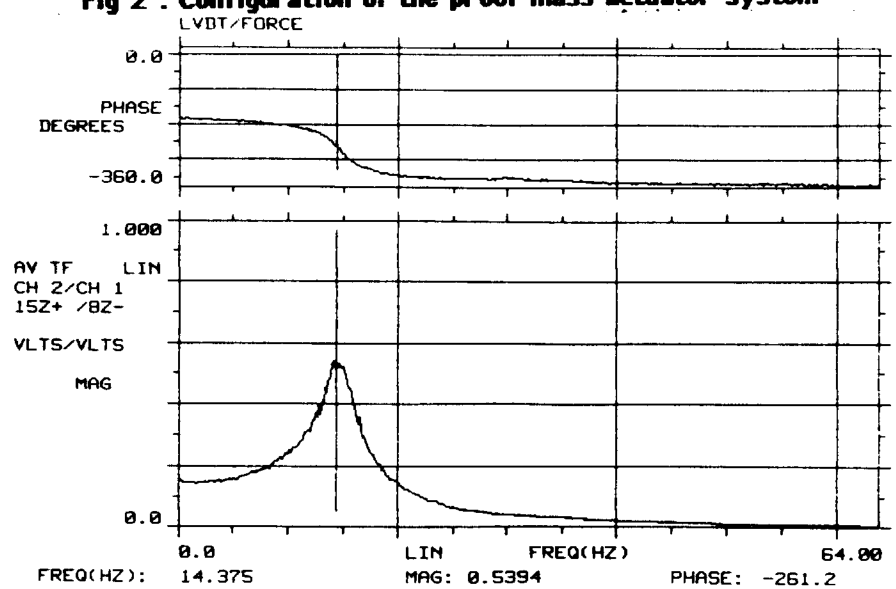

Fig.5 : Frequency Response function of the LVDT signal of the Proof-mass-actuator tuned to 14.4 Hz

ORIGINAL PAGE IS
OF POOR QUALITY

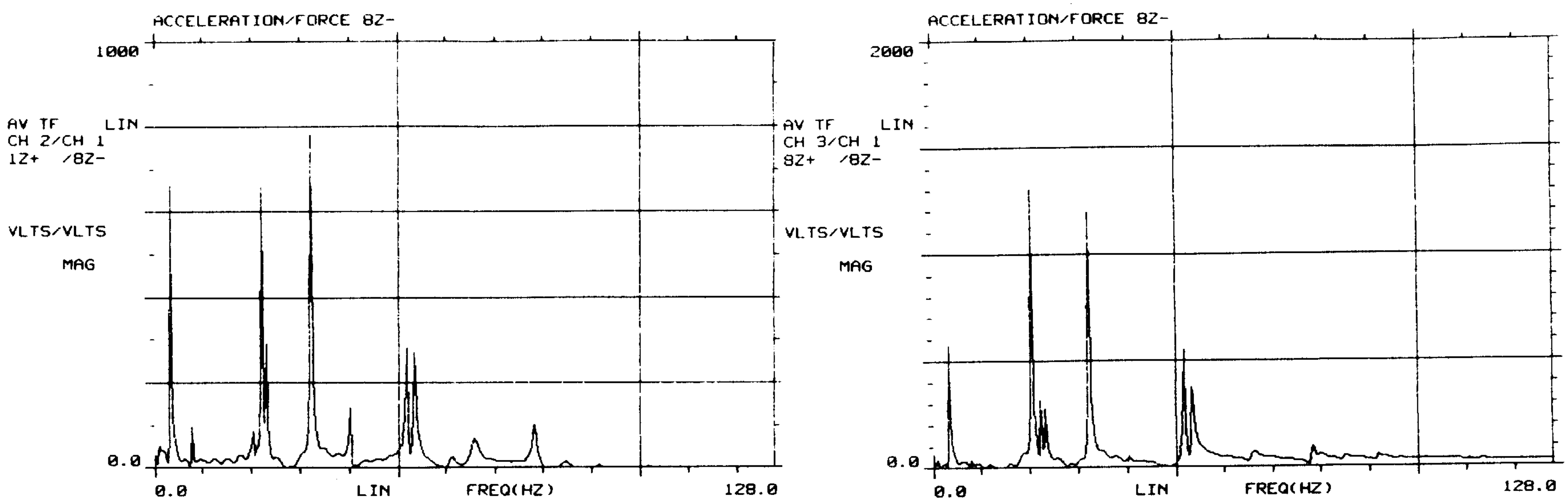

Fig.3 : Transfer function of the uncontrolled structure

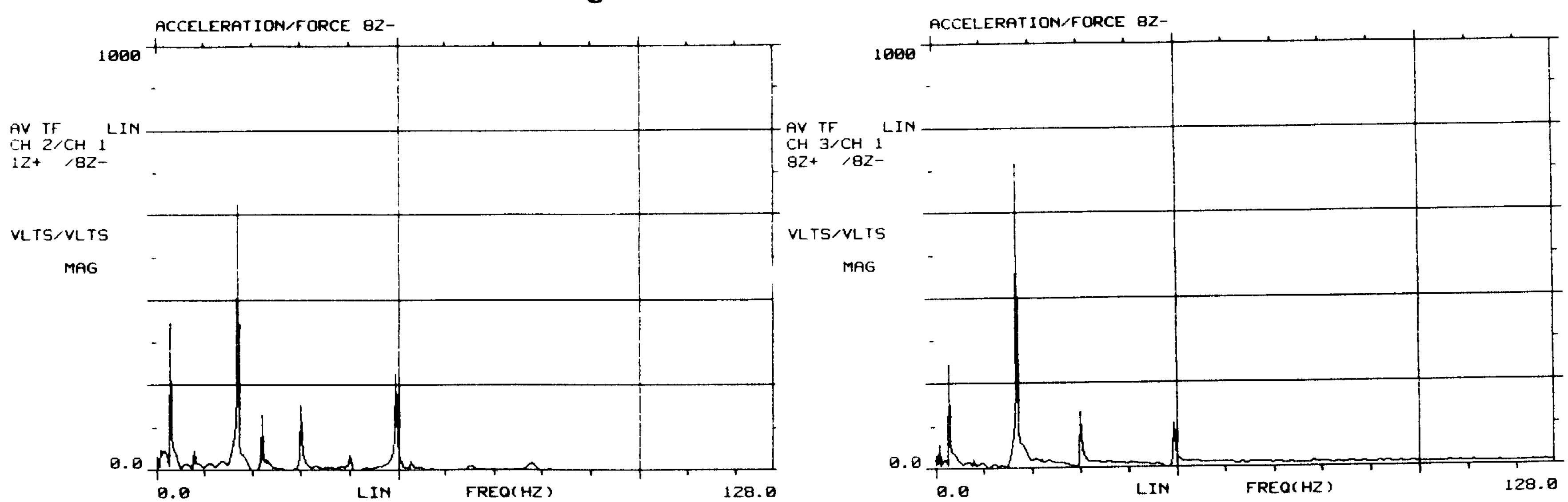

Fig.4 : Transfer function of the uncontrolled structure with parasitic mass

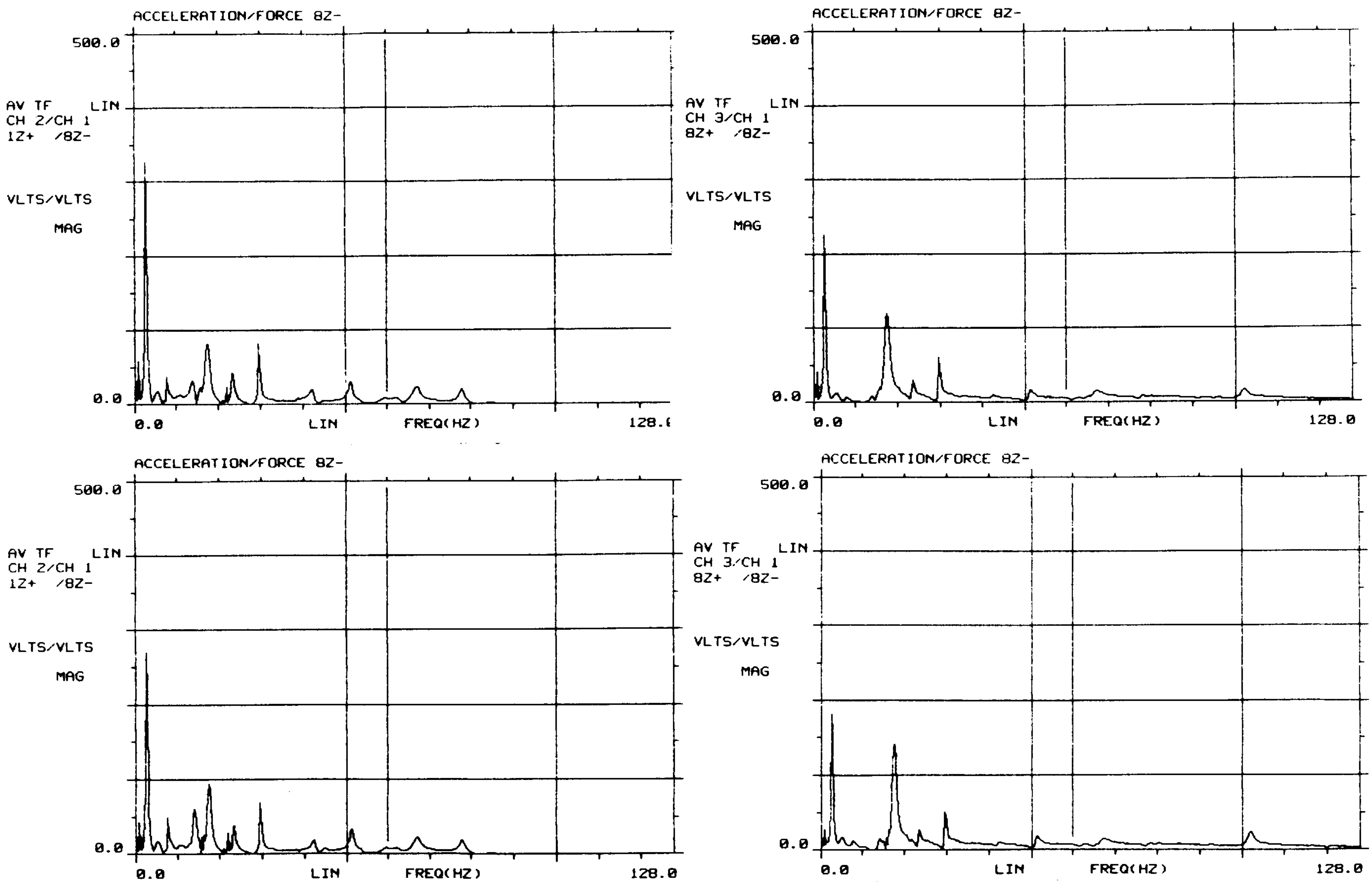

Fig.6 : Response of the passively controlled structure (top) and the actively controlled structure (bottom)

N90-23036

Simulation Studies Using Multibody Dynamics Code DART

James E. Keat
Photon Research Associates, Inc.

Abstract

DART is a multibody dynamics code developed by Photon Research Associates for the Air Force Astronautics Laboratory (AFAL). The code is intended primarily to simulate the dynamics of large space structures, particularly during the deployment phase of their missions. DART integrates nonlinear equations of motion numerically. The number of bodies in the system being simulated is arbitrary. The bodies' interconnection joints can have an arbitrary number of degrees of freedom between 0 and 6. Motions across the joints can be large. Provision for simulating on-board control systems is provided. Conservation of energy and momentum, when applicable, are used to evaluate DART's performance.

After a brief description of DART, the paper describes studies made to test the program prior to its delivery to AFAL. Three studies are described. The first is a large angle reorientating of a flexible spacecraft consisting of a rigid central hub and four flexible booms. Reorientation was accomplished by a single-cycle sine wave shape torque input. In the second study, an appendage, mounted on a spacecraft, was slewed through a large angle. Four closed-loop control systems provided control of this appendage and of the spacecraft's attitude. The third study simulated the deployment of the rim of a bicycle wheel configuration large space structure. This system contained 18 bodies. An interesting and unexpected feature of the dynamics was a pulsing phenomena experienced by the stays whose playout was used to control the deployment.

The paper concludes with a short description of the current status of DART.